Duality relation for the Maxwell system

F. Zolla[1] and S. Guenneau[2,*]
[1]*Institut Fresnel, UMR 6133, Faculté de Saint Jérôme, Case 162, 13397 Marseille Cedex 20, France*
[2]*Department of Mathematical Sciences, University of Liverpool, Liverpool L69 3BX, United Kingdom*
(Received 26 June 2002; published 24 February 2003)

This paper is intended to establish a link between the vector Maxwell system for three-dimensional (3D) and 2D finite photonic crystals in the low-frequency limit. For this, we generalize the classical results of Keller and Dykhne (chessboard problem) to periodic media described by piecewise continuous permittivity profiles: our theorem enlights the result of Mendelson (polycrystalline and multiphase media) in the framework of homogenization theory of elliptic operators. *In fine*, we give illustrative examples by using both integral equation and variational approaches via the so-called method of fictitious charges and finite-element method.

DOI: 10.1103/PhysRevE.67.026610 PACS number(s): 41.20.−q, 42.25.−p, 78.20.Bh, 41.20.Cv

I. INTRODUCTION

Some mathematical works devoted to the theory of composites go back to Wiener [1] by interchanging the roles of the background and matrix in the Lorentz-Lorenz formula. A classical theorem is that of Keller [2], which found a relation between the transverse effective conductivity of an array of cylinders and the conductivity when the phases are interchanged. The essence of Keller's theorem is that if in a two-dimensional (2D) potential problem for Laplace's equation u is a solution for a problem with one type of inclusion, then its Cauchy-Riemann partner v is the solution for the problem with the dielectric constant inverted and the electric field rotated by 90°. In 1970, Dykhne [3], using the fact that a divergence-free field when rotated locally at each point by 90° produces a curl-free field and vice versa could generalize Keller's result to isotropic multiphase and polycrystalline media. He noted that the duality relations implied exact formulas for the conductivity of phase-interchange-invariant two-phase media (such as checkerboards) and for polycrystals constructed from a single crystal. In Sec. III, we generalize the results of Keller [2], Nevard and Keller [4], and Dykhne [3]: we express the homogenized permittivity of a two-dimensional electrostatic problem in terms of the homogenized inverse permittivity up to a rotation of 90°. In the particular case of a checkerboard, i.e., a planar body of square symmetry characterized by a piecewise constant permittivity which takes the values ε_1 and ε_2, it can be then deduced the well-known formula [3]

$$\varepsilon_{\mathrm{eff}}=\sqrt{\varepsilon_1\varepsilon_1}.$$

This formula has been generalized by Kozlov in the random case and also the asymptotic behavior of $\varepsilon_{\mathrm{eff}}$ when ε_1 is small in term of percolation thresholds [5]. This formula was independently derived by Golden and Papanicolaou [6].

The pioneering works of Keller and Dykhne stimulated a large body of research: Berdichevski [7] derived an exact formula for the effective shear modulus of a checkerboard of two incompressible phases. The duality and phase interchange relations of Berdichevski were extended to anisotropic composite materials by Helsing, Milton, and Movchan [8] together with numerical results of high accuracy and Nemat-Nasser and Ni [9] obtained duality transformations for three-dimensional anisotropic bodies with stress and strain fields independent of the x_3 coordinate. Milton and Movchan [10] found an equivalence between planar elasticity problems and antiplane elasticity problems in inhomogeneous bodies. These results and additional duality relations were then discussed in detailed by Helsing, Milton, and Movchan [8]. A plethora of three-dimensional exact relations from pyroelectricity to thermopiezoelectric composites have recently been given by Grabovsky, Milton, and Sage [11].

Among other things, when no explicit formulas are available, it is an important matter to have *a priori* estimates on the effective matrix in term of the statistical properties of each component of the composite. This is the so-called theory of bounds which motivated a lot of contributions in several fields of physics, mechanics, and mathematics. The pioneering work was done by Hashin and Shtrikman in [12] where a complete description of all possible effective tensors was derived. This result was proved later by Tartar [13] who extended the result to the anisotropic case. Then many papers appeared in the literature among them, of which we may quote Benveniste [14] who obtained bound results in piezoelectricity and Francfort [15] who made a correspondence between the equations of incompressible elasticity and the duality relations for conductivity.

To conclude, the rigorous mathematical theory of the homogenization of elliptic operators with random coefficients proposed by Jikov, Kozlov, and Oleinik [16] is closely related to the Bergman-Milton theory of bounds [17–21] who obtained some bounds for the effective modulli of periodic and random structures.

II. LOW-FREQUENCY LIMIT OF THE VECTOR MAXWELL SYSTEM

The homogenization of 3D dielectric photonic crystals has been independently performed by Ke-Da *et al.* with the Rayleigh method (two-phase media with spherical inclusions) [22] and by Guenneau and Zolla with the multiple-

*FAX: +44 (0) 151 794 4061
Electronic address: guenneau@liverpool.ac.uk

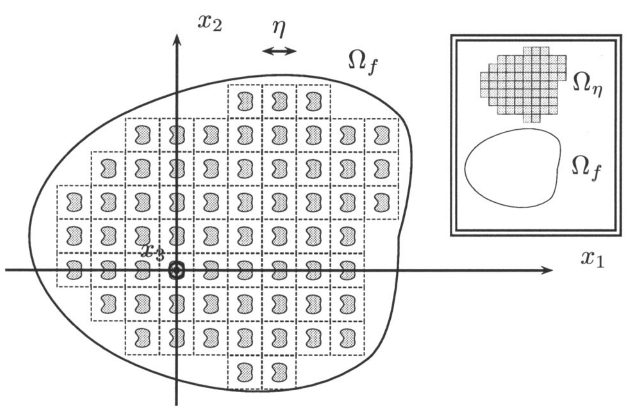

FIG. 1. The fixed set Ω_f and its "scaffolding" Ω_η for a fixed η.

scale method (media described by coercive and bounded permittivity profiles) [23]. The last authors use a limit analysis technique in which one lets the period η tend to-zero and, hence, the number of elementary cells to infinity, while keeping the wavelength $\lambda = 2\pi/k_0$ and the domain Ω_f containing the cells fixed (see Fig. 1).

Moreover, an oscillating magnetic field $\mathbf{H}_\eta$ is defined as the unique solution of the problem $(\mathcal{P}_\eta^{\mathbf{H}})$ in $[L^2_{\text{loc}}(\mathbb{R}^3)]^3$:

$$(\mathcal{P}_\eta^{\mathbf{H}})\begin{cases}\text{(i)} & \text{rot}(\varepsilon_\eta^{-1}\text{rot }\mathbf{H}_\eta) - k_0^2\mathbf{H}_\eta = 0,\\ \text{(ii)} & \text{div}\,\mathbf{H}_\eta = 0,\end{cases}$$

where the diffracted magnetic field $\mathbf{H}_\eta^d \overset{\text{def}}{=} \mathbf{H}_\eta - \mathbf{H}_{\text{inc}}$ satisfies Silver-Müller radiation conditions: namely,

$$\mathbf{H}_\eta^d = O\left(\frac{1}{|\mathbf{x}|}\right), \quad \frac{\mathbf{x}}{|\mathbf{x}|}\times\text{rot }\mathbf{H}_\eta^d + ik_0\mathbf{H}_\eta^d = o\left(\frac{1}{|\mathbf{X}|}\right),$$

and where $\varepsilon_\eta(\mathbf{x}) = \varepsilon(\mathbf{x}/\eta)$, ε being Y^3 periodic $(Y \overset{\text{def}}{=}]0,1])$. It can be proved that $\mathbf{H}_\eta$ has a two-scale expansion of the form

$$\forall \mathbf{x} \in \Omega_f,$$

$$\mathbf{H}_\eta(\mathbf{x}) = \mathbf{H}_0\left(\mathbf{x}, \frac{\mathbf{x}}{\eta}\right) + \eta\mathbf{H}_1\left(\mathbf{x}, \frac{\mathbf{x}}{\eta}\right) + \eta^2\mathbf{H}_2\left(\mathbf{x}, \frac{\mathbf{x}}{\eta}\right) + \cdots,$$

where $\mathbf{H}_i : \Omega_f \times Y^3 \mapsto \mathbb{C}^3$ is a function of six variables, independent of η, such that for all $\mathbf{x}$ in Ω_f, $\mathbf{H}_i(\mathbf{x},\cdot)$ is Y^3 periodic.

The salient consequence is that when η tends to zero, the $\mathbf{H}_\eta$ solution of the problem $(\mathcal{P}_\eta^{\mathbf{H}})$, converges in $[L^2_{\text{loc}}(\mathbb{R}^3)]^3$ to the unique solution $\mathbf{H}$ of the homogenized problem $(\mathcal{P}_{\text{hom}}^{\mathbf{H}})$ [23]:

$$(\mathcal{P}_{\text{hom}}^{\mathbf{H}})\begin{cases}\text{(iii)} & \text{rot}(\varepsilon_{\text{hom}}^{-1}\text{rot }\mathbf{H}) - k_0^2\mathbf{H} = 0,\\ \text{(ii)} & \text{div}\,\mathbf{H} = 0,\end{cases}$$

where the diffracted magnetic field $\mathbf{H}^d \overset{\text{def}}{=} \mathbf{H} - \mathbf{H}_{\text{inc}}$ satisfies Silver-Müller radiation conditions and where

$$\varepsilon_{\text{hom}} = \langle \varepsilon(\mathbf{y})[I - \nabla\mathbf{V}(y)]\rangle_{Y^3} \quad \text{in } \Omega_f,$$

the notation $\langle f\rangle_{Y^3}$ denoting the average of f in Y^3. Besides, $\mathbf{V} = (V_1, V_2, V_3)$, where V_j $(j \in \{1,2,3\})$ is the unique solution in $H^1_\sharp(Y^3)$ of the null mean of one of the three following problems $(\mathcal{K}_j)$ of electrostatic type:

$$(\mathcal{K}_j): -\text{div}\{\varepsilon(\mathbf{y})[\nabla(V_j(\mathbf{y}) - y_j)]\} = 0.$$

A. TM polarization deduced from the 3D case

When ε does not depend on the third component—namely, $\varepsilon(\mathbf{y}) = \varepsilon(y_1, y_2)$—we get

$$\varepsilon_{\text{hom}} = \begin{pmatrix} A_{\text{hom}} & & 0 \\ & & 0 \\ 0 & 0 & \langle\varepsilon\rangle_{Y^2}\end{pmatrix},$$

where A_{hom} is the 2×2 matrix given by

$$A_{\text{hom}} = \begin{pmatrix} \langle\varepsilon\rangle_{Y^2} - \langle\varepsilon\partial_1 V_1\rangle_{Y^2} & -\langle\varepsilon\partial_1 V_2\rangle_{Y^2} \\ -\langle\varepsilon\partial_2 V_1\rangle_{Y^2} & \langle\varepsilon\rangle_{Y^2} - \langle\varepsilon\partial_2 V_2\rangle_{Y^2}\end{pmatrix},$$

and V_j, $j \in \{1,2\}$, the unique solution in $H^1_\sharp(Y^2)/\mathbb{R}$ of

$$(\mathcal{P}_j^A): \text{div}\{\varepsilon(\mathbf{y})[\nabla(V_j(\mathbf{y}) - y_j)]\} = 0.$$

When Ω_f is invariant itself with respect to the third component and for the particular case of TM polarization $[\mathbf{H} = u(x_1, x_2)\mathbf{e}_3]$, it is clear that the result written above always holds.

B. TM polarization via 2D homogenization

Let us now consider the TM field $\mathbf{H}_\eta = u_\eta(x_1, x_2)\mathbf{e}_3$, where u_η is the unique solution of the scalar wave equation

$$\text{div}\left[\varepsilon^{-1}\left(\mathbf{x}, \frac{\mathbf{x}}{\eta}\right)\nabla u_\eta\right] + k_0^2 u_\eta = 0,$$

with Sommerfeld radiation conditions

$$u_\eta^d = O(1/\sqrt{|\mathbf{x}|}), \quad (u_\eta^d - ik_0\partial u_\eta^d/\partial x) = o(1/\sqrt{|\mathbf{x}|}).$$

When η tends to 0, u_η tends in $L^2_{\text{loc}}(\mathbb{R}^2)$ to the $u = u(x_1, x_2)$ unique solution of

$$\text{div}(A'_{\text{hom}}\nabla u) + k_0^2 u = 0,$$

where the diffracted field u^d satisfies the radiation conditions and where A'_{hom} is given by

$$A'_{\text{hom}} = \begin{pmatrix} \langle\varepsilon^{-1}\rangle_{Y^2} - \langle\varepsilon^{-1}\partial_1 V'_1\rangle_{Y^2} & -\langle\varepsilon^{-1}\partial_1 V'_2\rangle_{Y^2} \\ -\langle\varepsilon^{-1}\partial_2 V'_1\rangle_{Y^2} & \langle\varepsilon^{-1}\rangle_{Y^2} - \langle\varepsilon^{-1}\partial_2 V'_2\rangle_{Y^2}\end{pmatrix},$$

with V'_j the unique solution in $H^1_\sharp(Y^2)/\mathbb{R}$ of

$$(\mathcal{P}_j^B):\mathrm{div}\{\varepsilon^{-1}(\mathbf{y})[\nabla(V_j'(\mathbf{y})-y_j)]\}=0,$$

with $j\in\{1,2\}$.

III. DUALITY CORRESPONDENCES BETWEEN 3D AND 2D ANNEX PROBLEMS

We are facing a paradox: the annex problems in Secs. II A and II B involve, respectively, the permittivity and its inverse. To explain this discrepancy, we establish the following subtle property.

Proposition:

$$\mathrm{rot}\{\varepsilon_{\mathrm{hom}}^{-1}\mathrm{rot}[u(x_1,x_2)\mathbf{e}_3]\}$$
$$=-\mathrm{div}\left[R\left(\frac{\pi}{2}\right)A_{\mathrm{hom}}^{-1}R\left(-\frac{\pi}{2}\right)\nabla u\right]\mathbf{e}_3,$$

where $R(\pi/2)$ is the rotation matrix of angle $\pi/2$: namely,

$$R(\pi/2)=\begin{pmatrix}0&1\\-1&0\end{pmatrix}.$$

Proof: Let M be a symmetric matrix defined as

$$M=\begin{pmatrix}m_{11}&m&0\\m&m_{22}&0\\0&0&m_{33}\end{pmatrix}=\begin{pmatrix}\tilde{M}&0\\0&m_{33}\end{pmatrix};$$

we get

$$\mathrm{rot}\{M\ \mathrm{rot}[u(x_1,x_2)\mathbf{e}_3]\}=-\left[\frac{\partial}{\partial x_1}\left(m_{22}\frac{\partial u}{\partial x_1}-m\frac{\partial u}{\partial x_2}\right)\right.$$
$$\left.+\frac{\partial}{\partial x_2}\left(m_{11}\frac{\partial u}{\partial x_2}-m\frac{\partial u}{\partial x_1}\right)\right]\mathbf{e}_3.$$

Furthermore, let M' be defined as

$$M'=\begin{pmatrix}m_{11}'&m_{12}'\\m_{21}'&m_{22}'\end{pmatrix},$$

we have

$$\mathrm{rot}\{M\ \mathrm{rot}[u(x_1,x_2)\mathbf{e}_3]\}=-\mathrm{div}(M'\nabla u)\mathbf{e}_3,$$

if and only if

$$m_{11}'\frac{\partial u}{\partial x_1}+m_{12}'\frac{\partial u}{\partial x_2}=m_{22}\frac{\partial u}{\partial x_1}-m\frac{\partial u}{\partial x_2},$$

$$m_{21}'\frac{\partial u}{\partial x_1}+m_{22}'\frac{\partial u}{\partial x_2}=m_{11}\frac{\partial u}{\partial x_2}-m\frac{\partial u}{\partial x_1},$$

which is true if $M'=R(\pi/2)\tilde{M}R(-\pi/2)$. As a conclusion, the results found in Secs. II A and II B are consistent if and only if

$$A_{\mathrm{hom}}'=R\left(\frac{\pi}{2}\right)A_{\mathrm{hom}}^{-1}R\left(-\frac{\pi}{2}\right),$$

i.e.,

$$A_{\mathrm{hom}}'=\frac{A_{\mathrm{hom}}}{\det(A_{\mathrm{hom}})}.$$

This remarkable result—which was derived by Mendelson [24] and Nevard and Keller [4] in another homogenization framework—can be straightforwardly proved thanks to the following result due to Bouchitté [25,26].

Lemma. let A_{hom} and A_{hom}' be the homogenized matrices associated to w_j and w_j' ($j\in\{1,2\}$) unique solutions in $H_\sharp^1(Y^2)/\mathbb{C}$ of the four following problems:

$$\mathrm{div}[a(\mathbf{y})\nabla(y_j+w_j(\mathbf{y}))]=0,$$

$$\mathrm{div}[a'(\mathbf{y})\nabla(y_j+w_j'(\mathbf{y}))]=0,$$

where $a'=a^{-1}$. Then, we have

$$A_{\mathrm{hom}}'=\frac{A_{\mathrm{hom}}}{\det(A_{\mathrm{hom}})}.$$

Proof. We note that A_{hom} is given by the problem of minimization,

$$\frac{1}{2}A_{\mathrm{hom}}\xi\cdot\xi=\inf_{v(\mathbf{y})\in H_\sharp^1(Y^2)/\mathbb{C}}\left\{\frac{1}{2}\int_{Y^2}a(\mathbf{y})|\xi+\nabla v(\mathbf{y})|^2d^2\mathbf{y}\right\},$$

and A_{hom}^{-1} by its dual variational problem

$$\frac{1}{2}A_{\mathrm{hom}}^{-1}\xi^*\cdot\xi^*=\inf_{q(\mathbf{y})\in L_\sharp^2(Y^2)}\left\{\frac{1}{2}\int_{Y^2}a^{-1}(\mathbf{y})|\xi^*+q|^2d^2\mathbf{y},\right.$$

$$\left.\mathrm{div}_y q(\mathbf{y})=0,\quad\text{and}\quad\int_{Y^2}q(\mathbf{y})d^2\mathbf{y}=0\right\}.$$

Besides, we know that every divergence free field of $L_\sharp^2(Y^2)$ is the gradient of a function of $H_\sharp^1(Y^2)$, up to a rotation, provided its average is null [16]. Therefore, there exists a function $v\in H_\sharp^1(Y^2)$ (up to an additive constant) such that

$$q(\mathbf{y})=R(\nabla_y v(\mathbf{y})),$$

where $R\overset{\mathrm{def}}{=}R(\pi/2)$. Noting that

$$|\xi^*+q(\mathbf{y})|^2=|R\xi^*+Rq(\mathbf{y})|^2=|R\xi^*+\nabla v(\mathbf{y})|^2,$$

we get

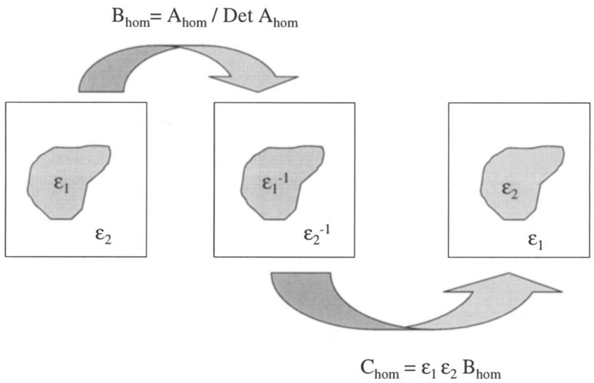

FIG. 2. Derivation of the effective matrix for an interchanged contrast between matrix and inclusions.

$$\frac{1}{2}A_{\text{hom}}^{-1}\xi^*\cdot\xi^* = \inf_{v(\mathbf{y})\in H^1_\sharp(Y^2)/\mathbb{C}}\left\{\frac{1}{2}\int_{Y^2}a^{-1}(\mathbf{y})|R\xi^*+\nabla v(\mathbf{y})|^2 d^2\mathbf{y}\right\}.$$

To conclude, we note that A'_{hom} is given by the following problem:

$$\frac{1}{2}A'_{\text{hom}}z\cdot z = \inf_{v(\mathbf{y})\in H^1_\sharp(Y^2)/\mathbb{C}}\left\{\frac{1}{2}\int_{Y^2}a^{-1}(\mathbf{y})|z+\nabla v(\mathbf{y})|^2 d^2\mathbf{y}\right\}.$$

IV. MISCELLANEOUS APPLICATIONS

In this section, we illustrate our duality result with a review of classical phase interchange identities such as the chessboard problem for two-phase media and its variants.

A. Two-phase media

Let Ω_f be a bounded photonic crystal filled with a periodic heterogeneous material with two optical indices $n_1=\sqrt{\varepsilon_1}$ and $n_2=\sqrt{\varepsilon_2}$. Thanks to the previous proposition, we can deduce from the computation of the effective matrix $A_{\text{hom}}([\varepsilon_1,\varepsilon_2])$ the effective matrix $A_{\text{hom}}([\varepsilon_2,\varepsilon_1])$ corresponding to the same structure with the reverse contrast (cf. Fig. 2). For this we use the general property

$$A_{\text{hom}}(\lambda\varepsilon)=\lambda A_{\text{hom}}(\varepsilon)\quad\text{for any fixed }\lambda\text{ in }\mathbb{C},$$

and the duality relation. Indeed, we have

$$A_{\text{hom}}([\varepsilon_2,\varepsilon_1])=\varepsilon_1\varepsilon_2 A_{\text{hom}}([\varepsilon_1^{-1},\varepsilon_2^{-1}])$$

and, then,

$$A_{\text{hom}}([\varepsilon_2,\varepsilon_1])=\frac{\varepsilon_1\varepsilon_2}{\det A_{\text{hom}}([\varepsilon_1,\varepsilon_2])}A_{\text{hom}}([\varepsilon_1,\varepsilon_2]).$$

In particular, for lossless dielectric materials, we have

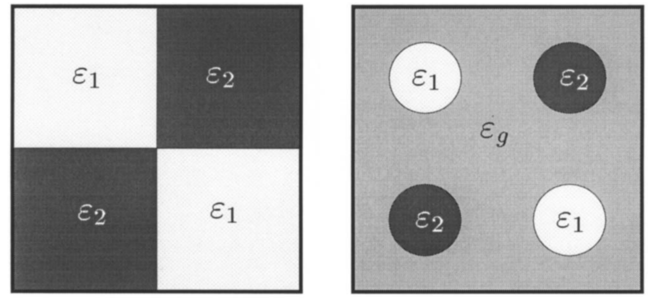

FIG. 3. Unit cell Y^2 for Dykhne's checkerboard problem [(a) on the left] and its variant [(b) on the right].

$$A_{\text{hom}}([\varepsilon_1,\varepsilon_2])=R(\varphi)\begin{pmatrix}\varepsilon_M & 0\\ 0 & \varepsilon_m\end{pmatrix}R(-\varphi),$$

where $R(\varphi)$ is the rotation matrix of angle φ and where $\varepsilon_M>\varepsilon_m$. The relation between the two matrices $A_{\text{hom}}([\varepsilon_1,\varepsilon_2])$ and $A_{\text{hom}}([\varepsilon_2,\varepsilon_1])$ leads to the following property:

$$A_{\text{hom}}([\varepsilon_2,\varepsilon_1])=R(\varphi)\begin{pmatrix}\varepsilon'_M & 0\\ 0 & \varepsilon'_m\end{pmatrix}R(-\varphi),$$

with $\varepsilon'_M=\varepsilon_1\varepsilon_2/\varepsilon_m$ and $\varepsilon'_m=\varepsilon_1\varepsilon_2/\varepsilon_M$ (note that $\varepsilon'_M>\varepsilon'_m$).

B. Checkerboard problem

The checkerboard problem is obviously a two-phase problem [cf. Fig. 3(a)]. Besides, for a squared symmetry (it is the case for the checkerboard problem up to a translation) it can be easily proved that A_{hom} is equal to $R(\pi/2)A_{\text{hom}}R(-\pi/2)$ and consequently A_{hom} is proportional to the identity matrix (the effective permittivity in TM polarization is therefore isotropic):

$$A_{\text{hom}}([\varepsilon_1,\varepsilon_2])=A_{\text{hom}}([\varepsilon_2,\varepsilon_1])=a_{\text{hom}}I.$$

The previous result shows that

$$A_{\text{hom}}([\varepsilon_1,\varepsilon_2])=\frac{\varepsilon_1\varepsilon_2}{\det A_{\text{hom}}([\varepsilon_1,\varepsilon_2])}A_{\text{hom}}([\varepsilon_1,\varepsilon_2]),$$

and consequently $\det A_{\text{hom}}([\varepsilon_1,\varepsilon_2])=a_{\text{hom}}^2=\varepsilon_1\varepsilon_2$. Finally, we rediscover the result of Dykhne [3]:

$$A_{\text{hom}}=\sqrt{\varepsilon_1\varepsilon_2}I.$$

C. Variant of the checkerboard problem

Let us now consider a three-phase problem characterized by three permittivities ε_1, ε_2, and ε_g [cf. Fig. 3(b)]. The associated homogenized matrix is then $A_{\text{hom}}([\varepsilon_1,\varepsilon_2,\varepsilon_g])$. Using the technics described above, we get the relation

$$A_{\text{hom}}\left(\left[\varepsilon_2,\varepsilon_1,\frac{\varepsilon_1\varepsilon_2}{\varepsilon_g}\right]\right)=\frac{\varepsilon_1\varepsilon_2 A_{\text{hom}}([\varepsilon_1,\varepsilon_2,\varepsilon_g])}{\det A_{\text{hom}}([\varepsilon_1,\varepsilon_2,\varepsilon_g])},$$

which becomes very interesting if $\varepsilon_g = \sqrt{\varepsilon_1 \varepsilon_2}$. In particular, when the cell Y^2 has a squared symmetry as shown in Fig. 3, we obtain

$$A_{\text{hom}} = \sqrt{\varepsilon_1 \varepsilon_2} I = \varepsilon_g I.$$

It is worth noting that considering a four-homogeneous-medium problem characterized by four permittivities ε_1, ε_2 and ε_{g1}, ε_{g2} deduced from Figs. 3(a) and 3(b) by substituting Fig. 3(b) into Fig. 3(a) would merely lead to

$$A_{\text{hom}}\left(\left[\varepsilon_2, \varepsilon_1, \frac{\varepsilon_1 \varepsilon_2}{\varepsilon_{g1}}, \frac{\varepsilon_1 \varepsilon_2}{\varepsilon_{g2}}\right]\right) = \frac{\varepsilon_1 \varepsilon_2 A_{\text{hom}}([\varepsilon_1, \varepsilon_2, \varepsilon_{g1}, \varepsilon_{g2}])}{\det A_{\text{hom}}([\varepsilon_1, \varepsilon_2, \varepsilon_{g1}, \varepsilon_{g2}])},$$

which only simplifies in the trivial case $\varepsilon_{g1} = \varepsilon_{g2} = \sqrt{\varepsilon_1 \varepsilon_2}$. Nevertheless, one can still imagine some two phase variants of Dykhne's checkerboard problem as was done by Schulgasser [27,28] who noticed that there are some anisotropic two-dimensional microstructures such that interchanging the phases produces the same effect as rotating the structure by 90° and thereby leads to Dykhne's formula.

V. NUMERICAL RESOLUTION OF THE ANNEX PROBLEMS

A. Method of fictitious charges as applied to the two-phase media

To illustrate our purpose, we now make use of the method of fictitious charges (its dynamic analogue is the method of fictitious sources [29]), which takes benefit of the piecewise constant permittivity and of its periodicity to solve numerically the annex problems.

1. Preliminary remarks

In most applications, one has just to consider a two-valued piecewise constant permittivity in the unique cell Y^2 and, more precisely, the relative permittivity yields ε_2 in what one usually calls the scatterer S and ε_1 elsewhere. Consequently, the problem we are dealing with is only defined by two complexes and the shape of the scatterers Γ such as in the example shown in Fig. 4 (in other words, the scatterers lie in the volume area, support of the above function).

It is therefore easy to show [23] that in this case the resolution of the two annex problems ($\mathcal{K}_j$) introduced in the fundamental theorem as mentioned earlier amounts to looking for the function V_j solutions of the following system where derivatives are taken in the usual sense:

$$\Delta V_i = 0 \quad \text{in} \quad Y^2 \backslash \Gamma,$$

$$\left[\varepsilon \frac{\partial V_i}{\partial n}\right]_\Gamma = -[\varepsilon]_\Gamma n_i, \tag{1}$$

$$[V_i]_\Gamma = 0,$$

with

$$\varepsilon = \begin{cases} \varepsilon_1 & \text{in } \Omega_1, \\ \varepsilon_2 & \text{in } \Omega_2, \end{cases} \tag{2}$$

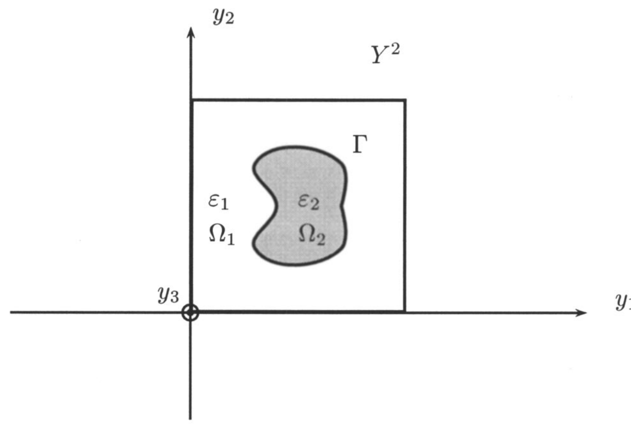

FIG. 4. Unit cell Y^2 with a scatterer characterized by the curve Γ.

where $[f]_\Gamma$ denotes the jump of f across the boundary Γ, and n_i, $i \in \{1,2,3\}$, denotes the projection on the axis $\mathbf{e}_i$ of a normal of Γ. Moreover, the calculus of the anisotropic permittivity can be simplified. Indeed, it had been shown [23] that the coefficients $\varphi_{i,j}$ are given by the following simple integral:

$$\varphi_{i,j} = [\varepsilon]_\Gamma \int_\Gamma V_i n_j ds. \tag{3}$$

Let us remark that V_i is well defined on Γ because it does not suffer a jump across the boundary of the scatterer. This last formula is very important for numerical implementations: it is not necessary to compute the gradient of V_i (which gives rise to numerical inaccuracy) to perform the calculus of the homogenized permittivity.

2. Some examples for the TM polarization

The method of fictitious charges as applied to the annex problem described above consists in representing the potential by an approximate potential with an error as small as we want. This approximate potential is created by two families of charges (they do not actually exist). The first ones are located in Ω_1 and radiate in Ω_2, and the second ones are located in Ω_2 and radiate in Ω_1. Each of these charges verifies a Laplace equation in Y^2 with periodic conditions, and they are chosen such that the potential verifies the boundary conditions that appear in Eq. (1). It is worth noting that we determine the amplitudes thanks to a least-square method. This method allows us to check the validity of the approximate potential and thus the one of the approximate homogenized permittivity. In order to illustrate the capabilities of our method, we compute the homogenized permittivity with elliptical scatterers described in Fig. 5.

In such a case, in the TE polarization ε_{hom} is merely the average of the permittivity in the cell Y^2 and thus does not depend on the angle θ. Conversely, in the TM polarization,

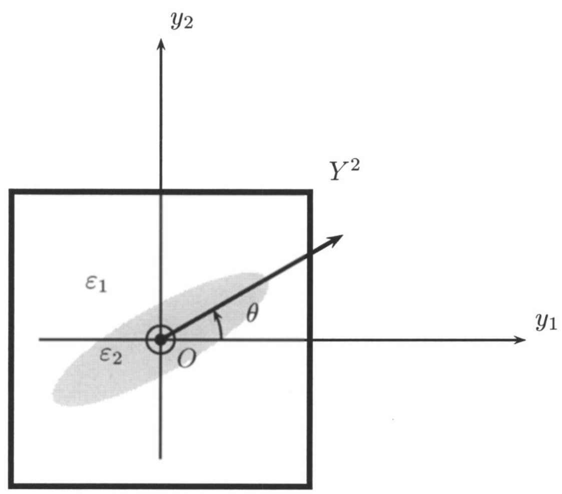

FIG. 5. Unit cell $Y^2 =]0;1]^2$ with an elliptical scatterer characterized by the major and the minor axes a and b and the angle θ.

A_{hom} is described by three coefficients φ_{11}, φ_{22}, and ψ, which depend on the angle θ:

$$A_{\text{hom}}(\theta) = \begin{pmatrix} \varphi_{11}(\theta) & \psi(\theta) \\ \psi(\theta) & \varphi_{22}(\theta) \end{pmatrix}. \tag{4}$$

Besides, when the permittivity ε_1 and ε_2 are real these coefficients are obviously real and consequently A_{hom} can write as follows:

$$A_{\text{hom}}(\theta) = R(\varphi) \begin{pmatrix} \varepsilon_M(\theta) & 0 \\ 0 & \varepsilon_m(\theta) \end{pmatrix} R(-\varphi), \tag{5}$$

where $R(\varphi)$ is an angle φ rotation matrix and ε_M and ε_m are chosen in such a way that $\varepsilon_M > \varepsilon_m$. In Figs. 6–8, we show the curves of $\varepsilon_{\text{ave}} = \langle \varepsilon \rangle$, ε_m, ε_M, and $\varepsilon_{\text{har}} = \langle \varepsilon^{-1} \rangle^{-1}$ versus θ for an elliptical scatterer of equation, $x_1^2/a + x_2^2/b = 1$ with $a = 0.4$ and $b = 0.2$ (normalized by the unit length of Y^2) and for the relative permittivities $\varepsilon_1 = 1$ and $\varepsilon_2 = 4$, 9, and 16. Finally, we draw φ versus θ for the same ellipse (cf. Fig. 9). Special attention must be drawn about the fact that this last curve only depends on the geometry. It is the same curve whatever the relative permittivities ε_1 and ε_2.

B. Multiphase media

In this section, we give a numerical illustration of the duality correspondence between the annex problems $(\mathcal{P}_j^A)$ $(\mathcal{P}_j^B)$ of Secs. II A and II B for multiphase media (ε is a continuous function), thanks to the finite-element method.

Multiplying $\text{div}_y[\varepsilon \nabla_y (V_i - y_i)]$ by V_j in $(\mathcal{P}_j^A)$, $j \in \{1,2\}$, and integrating by parts over the basic cell Y^2 leads to the weak formulation

$$\langle \varepsilon(\mathbf{y}) [\nabla_y (V_i - y_i)] \cdot \nabla V_j \rangle_{Y^2} = 0. \tag{6}$$

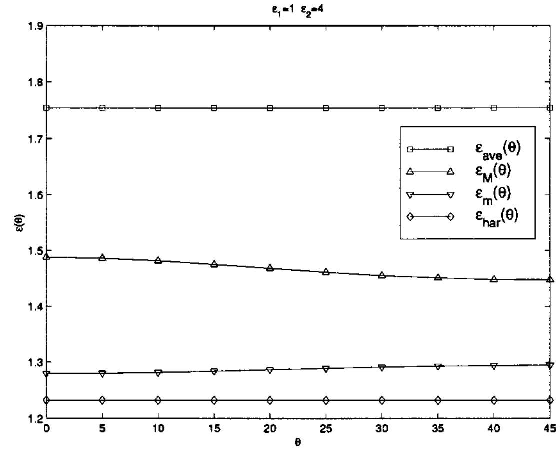

FIG. 6. Maximum (ε_M) and minimum (ε_m) eigenvalues of the tensor of permittivity A_{hom} in $H_\parallel$ for elliptical scatterers versus the orientation of these ellipses (θ, expressed in degrees). The ellipsis is characterized by the equation $x_1^2/a + x_2^2/b = 1$ with $a = 0.4$ and $b = 0.2$ (normalized by the unit length of Y^2) and filled with a dielectric of relative permittivity $\varepsilon_2 = 4$. In the same figure we draw the arithmetic average $\varepsilon_{\text{ave}} = \langle \varepsilon \rangle$ and the harmonic average $\varepsilon_{\text{har}} = \langle \varepsilon^{-1} \rangle^{-1}$.

To get the corresponding variational equation for $(\mathcal{P}_j^B)$, one has to replace ε by ε^{-1}. In the discrete formulation the basic cell is meshed with triangles and node elements are used for the scalar fields V_i:

$$V_i = \sum_k^n \beta_i^k w_k^n(x,y) \quad \text{in} \quad Y^2, \tag{7}$$

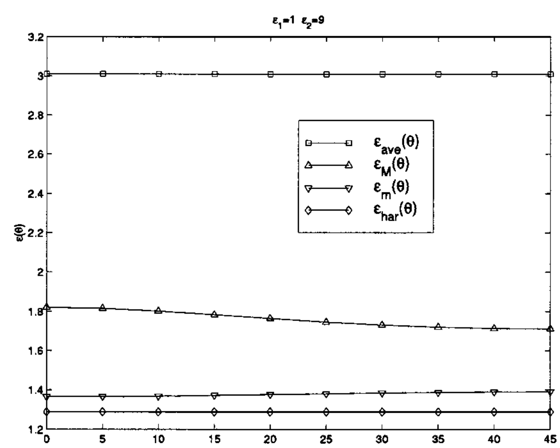

FIG. 7. Maximum (ε_M) and minimum (ε_m) eigenvalues of the tensor of permittivity A_{hom} in $H_\parallel$ for elliptical scatterers versus the orientation of these ellipses (θ, expressed in degrees). The ellipsis is characterized by the equation $x_1^2/a + x_2^2/b = 1$ with $a = 0.4$ and $b = 0.2$ (normalized by the unit length of Y^2) and filled with a dielectric of relative permittivity $\varepsilon_2 = 9$. In the same figure we draw the arithmetic average $\varepsilon_{\text{ave}} = \langle \varepsilon \rangle$ and the harmonic average $\varepsilon_{\text{har}} = \langle \varepsilon^{-1} \rangle^{-1}$.

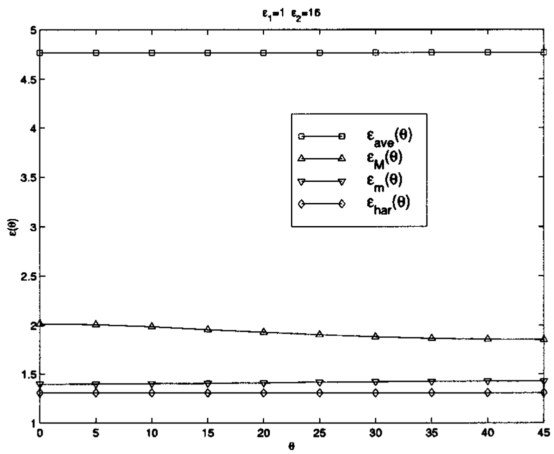

FIG. 8. Maximum (ε_M) and minimum (ε_m) eigenvalues of the tensor of permittivity $A_{\rm hom}$ in $H_\parallel$ for elliptical scatterers versus the orientation of these ellipses (θ, expressed in degrees). The ellipsis is characterized by the equation $x_1^2/a+x_2^2/b=1$ with $a=0.4$ and $b=0.2$ (normalized by the unit length of Y^2) and filled with a dielectric of relative permittivity $\varepsilon_2=9$. In the same figure we draw the arithmetic average $\varepsilon_{\rm ave}=\langle\varepsilon\rangle$ and the harmonic average $\varepsilon_{\rm har}=\langle\varepsilon^{-1}\rangle^{-1}$.

where β_i^k denotes the nodal value of the component V_i of the multiscalar potential $\mathbf{V}$. Besides, w_k^n are basis functions of first-order finite elements. The GETDP software [30] has been used to set up the finite-element problem with some periodicity conditions imposed on the field on opposite sides of the basic cell Y^2. From the numerical resolution of Eq. (6), we derive

$$A_{\rm hom}=\begin{pmatrix} 4.4078046 & -2.5388076\times10^{-5} \\ -2.5388076\times10^{-5} & 5.1888463 \end{pmatrix} \tag{8}$$

with $\langle\varepsilon\rangle_{Y^2}=5.374\,573\,4$ (see Fig. 10 for the associated eigenfield). We note that the off-diagonal terms are not

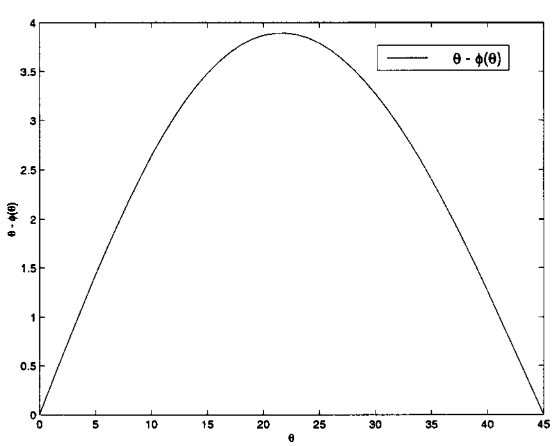

FIG. 9. Angle φ being the rotation of the optical axis and θ defining the orientation of the elliptical scatterer (both expressed in degrees), we draw the difference between φ and θ as a function of θ. This curve does not depend on neither the relative permittivity ε_1 nor ε_2.

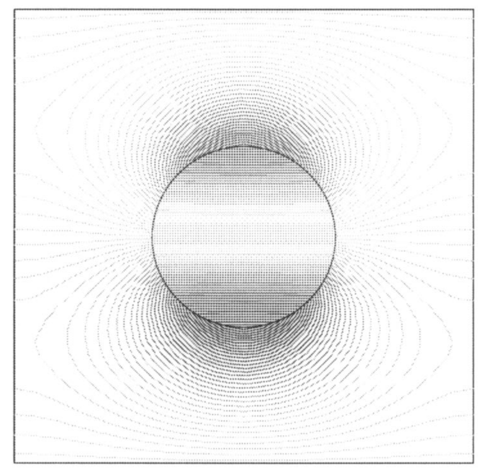

FIG. 10. Isovalues of the component V_1 of the (dimensionless) multiscalar field $\mathbf{V}$ in a unit basic cell Y^2, corresponding to a microstructure of silica [relative permittivity $\varepsilon_1(x,y)=1.25$] with a periodic arrangement of circular inclusions filled with a material described by a continuous profile of relative permittivity $\varepsilon_2(x,y)=2+2\sqrt{(x-0.5)^2/0.5+(y-0.5)^2/0.2}$.

strictly null: this artificial anisotropy induced by the mesh of the structure indicates the order of magnitude of the numerical error. Let us emphasize that we can deal with every type of geometry in the basic cell and that ε can even be a tensor (provided it is symmetric, coercive, and bounded).

VI. MULTISCALE EXPANSION VERSUS MULTIPOLE METHOD

If we now consider a 2D periodic two-phase medium with circular inclusions, our results give also some information on the corresponding effective properties of the material derived as a limit case of the multipole expansion (long-wavelength and dilute composite). In the classical book by Bensoussan, Lions, and Papanicolaou [31], a lemma states that when it exists, the tensor

$$\varepsilon^{-1}_{{\rm hom},pq}=\frac{1}{2}\,\frac{\partial\omega_1^2}{\xi_p\xi_q}(0), \tag{9}$$

defines the effective mass tensor of the first band, ξ denoting the so-called Bloch vector. It is worth noting that there is therefore no contradiction between our duality results and the work by McPhedran *et al.* [32], which states that the first dynamic correction to the Lorentz-Lorenz formula damages the symmetry of Keller's theorem. Besides, we have no such restriction as a small inclusion.

Also, some effective properties were obtained by Yardley *et al.* [33] where a uniform electrostatic field is imposed upon a rectangular array of elliptical cylinders embedded in a matrix of unit dielectric constants. These authors used a generalization of the Rayleigh's multipole technique to include geometries other than circles or spheres. They numerically verified Keller's reciprocal relationship [2] for this electrostatic problem. Our approach applies straightforwardly to the case of a rectangular basic cell, and our numerical results proved to be in good agreement with that of Yardley *et al.* [33]. Finally, some boundary collocation method was used by Lu [34] to study anisotropic effective conductivities of such rectangular arrays of elliptic cylinders when the aspect ratio of the ellipse and the edge length ratio of the array are varying. Here we emphasize that our numerical methods allow us to check the validity of Keller's reciprocal theorem for inclusions of arbitrary shape [with method of fictitious charges (MFC)] and with continuity profiles [with finite element method (FEM)], within less than 1%. Our algorithms are fast, accurate, and they are stable when the inclusions are close to touching (they can even touch the edges of the basic cell). Furthermore, we can treat the case of many inclusions in the unit cell and thereby have access to any kind of geometry for the array (e.g., hexagonal array).

VII. CONCLUSION

To our knowledge, this paper presents the first theoretical and numerical achievements of duality relations for the homogenized Maxwell system for noncircular inclusions (via the MFC) and continuous permittivity profiles (with FEM). The links with effective transport properties have been discussed. The authors are looking forward for analogous duality relations for ferromagnetic materials [35].

ACKNOWLEDGMENTS

Many thanks are due to Professor G. Bouchitté for providing the key result of lemma 2 as well as references on duality relations. The authors thank Professor A.B. Movchan and R. McPhedran for drawing their attention to the works of D. J. Bergman and G. Milton.

[1] O. Wiener, Abh. Math.-Phys. Kl. Saechs. Akad. Wiss. **509**(32), (1912).
[2] J. B. Keller, J. Math. Phys. **5**, 548 (1964).
[3] A. M. Dykhne, Zh. Eksp. Teor. Fiz. **59**, 110 (1970) [Sov. Phys. JETP **32**, 63 (1970)].
[4] J. Nevard and J. B. Keller, J. Math. Phys. **26**, 2761 (1985).
[5] S. M. Kozlov, Funkt. Anal. Prilozh. **2**, 101 (1984).
[6] K. Golden and G. Papanicolaou, Commun. Math. Phys. **90**, 473 (1983).
[7] V. L. Berdichevski, *Variational Principles in the Mechanics of Continuum Media* (Nauka, Moscow, 1983).
[8] J. Helsing, G. W. Milton, and A. B. Movchan, J. Mech. Phys. Solids **45**, 565 (1997).
[9] S. Nemat-Nasser and L. Ni, Int. J. Solids Struct. **32**, 467 (1995).
[10] G. W. Milton and A. B. Movchan, Proc. R. Soc. London, Ser. A **450**, 293 (1995).
[11] Y. Grabovsky, G. W. Milton, and D. S. Sage, Commun. Pure Appl. Math. **53**, 300 (2000).
[12] Z. Hashin and S. Shtrikman, J. Appl. Phys. **33**, 3125 (1962).
[13] L. Tartar, *Ennio de Giorgi Colloquium, Paris, 1983*, Research Notes in Mathematics, 125 (Pitman, Boston, 1985), pp. 168–169.
[14] Y. Benveniste, J. Mech. Phys. Solids **43**, 553 (1995).
[15] G. Francfort, Proc. R. Soc. Edinburgh, Sect. A: Math. **120**, 25 (1992).
[16] V. Jikov, S. Kozlov, and O. Oleinik, *Homogenization of Differential Operators* (Springer-Verlag, Berlin, 1995).
[17] G. W. Milton, Appl. Phys. Lett. **37**, 300 (1980).
[18] G. W. Milton, J. Appl. Phys. **52**, 5286 (1981).
[19] G. W. Milton, J. Appl. Phys. **52**, 5294 (1981).
[20] R. C. McPhedran and G. W. Milton, Appl. Phys. A: Solids Surf. **26**, 207 (1981).
[21] D. J. Bergman and D. Stroud, Solid State Phys. **46**, 147 (1992).
[22] Bao Ke-Da, C. G. Poulton, L. C. Botten, R. C. McPhedran, and N. A. Nicorovici, Physica B **279**, 162 (2000).
[23] S. Guenneau and F. Zolla, JEWA **14**, 529 (2000); PIER **27**, 91 (2000).
[24] K. S. Mendelson, J. Appl. Phys. **46**, 4740 (1975).
[25] G. Bouchitté (private communication).
[26] S. Guenneau, Ph.D. thesis, University of Provence, Marseille, 2001.
[27] K. Schulgasser, Int. Commun. Heat Mass Transfer **19**, 639 (1992).
[28] G. W. Milton, *The Theory of Composite*, Cambridge monographs on applied and computational mathematics No. 6 (Cambridge University Press, Cambridge, England, 2000).
[29] F. Zolla, R. Petit, and C. Cadilhac, J. Opt. Soc. Am. A **11**, 1087 (1994).
[30] P. Dular, C. Geuzaine, F. Henrotte, and W. Legros, IEEE Trans. Magn. **34**, 3395 (1998).
[31] A. Bensoussan, J. L. Lions, and G. Papanicolaou, *Asymptotic Analysis for Periodic Structures* (North-Holland, Amsterdam, 1978), p. 637.
[32] R. C. McPhedran, C. G. Poulton, N. A. Nicorovici, and A. B. Movchan, Proc. R. Soc. London, Ser. A **452**, 2231 (1996).
[33] J. G. Yardley, R. C. McPhedran, N. A. Nicorovici, and L. C. Botten, Phys. Rev. E **60**, 6068 (1999).
[34] Lu Shih-Yuan, J. Appl. Phys. **76**, 2641 (1994).
[35] S. Guenneau and F. Zolla (unpublished).